

P4.12

## EXAMINING RADAR 'SIDELOBE SPIKES' FOR SEVERE HAIL IDENTIFICATION

Kevin L. Manross<sup>1</sup>, Kiel L. Ortega<sup>1</sup> and Albert E. Pietrycha<sup>2</sup>

<sup>1</sup> *Cooperative Institute for Mesoscale Meteorology Studies, Univ. of Oklahoma, Norman, OK and NOAA/National Severe Storms Laboratory, Norman, OK*

<sup>2</sup> *NOAA/National Weather Service, Goodland, KS*

### 1. Introduction

Operational forecasters are faced with the challenge to produce highly accurate warnings during severe weather episodes. Warning quality includes a high probability of detection (POD), a low False Alarm Ratio (FAR), and sufficient lead time. Due to its ability to provide rapidly updating, highly spatial information to the forecaster, radar is a heavily relied on tool for diagnosing the potential presence of severe weather. Radar interrogation can fall into two general categories: qualitative and quantitative. Quantitative algorithms like the Mesocyclone Detection Algorithm (MDA) (Stumpf, et al. 1998) and Hail Detection Algorithm (HDA) (Witt, et al. 1998), to name just a few, mine radar data to produce numerical output about the strength or likelihood of a particular severe weather event like strong winds, hail, etc. Many quantitative algorithms follow from qualitative storm identification techniques. For example, areas of rotation within a storm were inferred by observing neighboring areas of inbound and outbound radial velocity with Doppler radar. After observing a repeatable pattern of rotation in Doppler radar data associated with tornadic events, researchers defined the mesocyclone (Donaldson 1970; Burgess 1976)

Not all qualitative identification techniques lend themselves to the development of quantitative algorithms. However, the ability to qualitatively identify features adds information to the forecaster about the severity of the storm and its associated weather. Features like the bounded weak echo region (BWER) provide an idea of the strength of the updraft of a storm (Lemon 1998a) and the three body scatter spike (TBSS) indicates the likely presence of large hail (Lemon 1998b). The overall goal of quantitative algorithm output or qualitative feature identification is to increase the forecaster's confidence in whether he or she needs to issue a warning and improve overall warning quality.

To aid in this effort of forecaster confidence, this paper examines a feature associated with radar sidelobe returns and its utility to diagnose the presence of severe hail ( $\geq 1$  in. dia.). It appears, from a limited number of samples, that there is good agreement between the presence of a sidelobe spike and the presence of severe hail at the ground. This paper continues with a definition of the sidelobe spike and the conditions which it is observed. After that, several cases where sidelobe spikes have been observed will be examined with respect to ground truth hail reports. Finally, some areas of future work will be discussed and conclusions from the current set of cases will be presented.

---

*Corresponding Author: Kevin L. Manross  
120 David L. Boren Blvd., Rm 3923, Norman, OK  
73072. Email: Kevin.Manross@noaa.gov*

### 2. Sidelobes and Sidelobe "Spike"

Not all radars suffer from significant sidelobes contamination. Bringi and Chandrasekar (2001) state that “Offset-feed parabolic reflector antennas are clearly superior in terms of sidelobe performance because feed and support strut blockages are eliminated.” Both they and Doviak and Zrnic (1993) blame the support struts for the feedhorn, as well as the radome, for causing significant sidelobes in the antenna pattern. The NEXRAD WSR-88D (Crum and Alberty, 1993) used by the National Oceanic and Atmospheric Administration’s (NOAA) National Weather Service (NWS) employs the strut and radome design that leads to sidelobes. This design is engineered such that the first sidelobe level is “less than or equal to -27 dB relative to the peak of the main lobe” and the first sidelobe occurs at approximately  $\pm 1.2^\circ$  off of the main lobe axis (Federal Handbook). This means that in order to detect a significant return through the first sidelobe, that return “must be stronger than the signal in the main lobe, by at least the two-way, first-sidelobe isolation (i.e., >50 dB). This requires a reflectivity gradient of greater than 50 dB per 1.2 degrees (greater than 40 dB degree<sup>-1</sup> sustained over about 2 degrees)” (Federal Handbook) (Figure 1). While the Federal Handbook suggests that this is a rare occurrence, Doviak and Zrnic (1993) states that these conditions are “not so uncommon”, and Bringi and Chandrasekar (2001) mention that such high reflectivity gradients “might occur in supercell hailstorms.” Doviak and Zrnic offer a useful illustration and description in their figure 7.27.

Sidelobe contamination is indeed a common occurrence as seen by operational forecasters. In fact the NWS Warning Decision Training Branch (WDTB) specifically mentions this type of sidelobe contamination in their

Distance Learning Operations Course (Figure 2) (WDTB 2010). With the implementation of 0.5 degree azimuth by 250 meter range “Super-Resolution” scanning strategies (Brown, et al. 2005), sidelobe spikes should be more obvious to radar users.

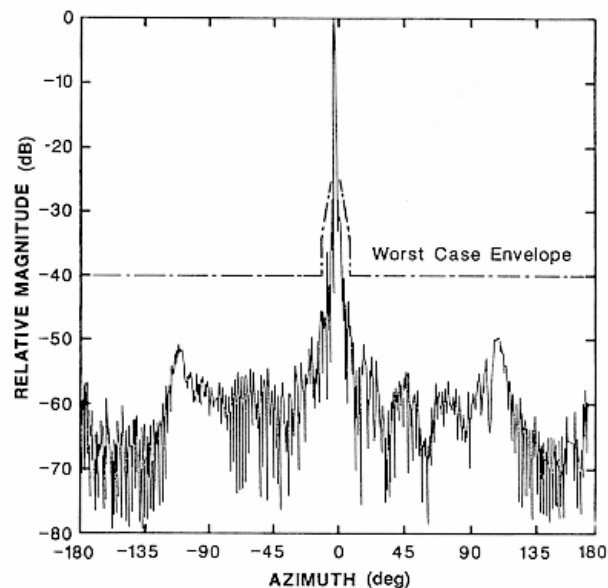


**Figure 1. “Typical antenna pattern for the WSR-88D and worst case sidelobe envelope” (from Federal Handbook Figure 3-18)**

The sidelobe spike is different than the TBSS both in how it forms and its appearance on radar. As described above, the sidelobe spike is a result of power return in usually the first sidelobe of the radar beam in the presence of a strong reflectivity gradient. Enough power is returned via the sidelobe, but it “appears” in the main lobe, but at a much weaker level, approximately 50 dB less than if the highly reflective area were sampled by the main lobe (valid for the WSR-88D). So a 60 dBZ area sampled by the sidelobe should appear as an approximately 10 dBZ area in the main lobe under these conditions. The sidelobe spike appears on radar as an elongation of weak return that extends azimuthally from the strong reflectivity core.

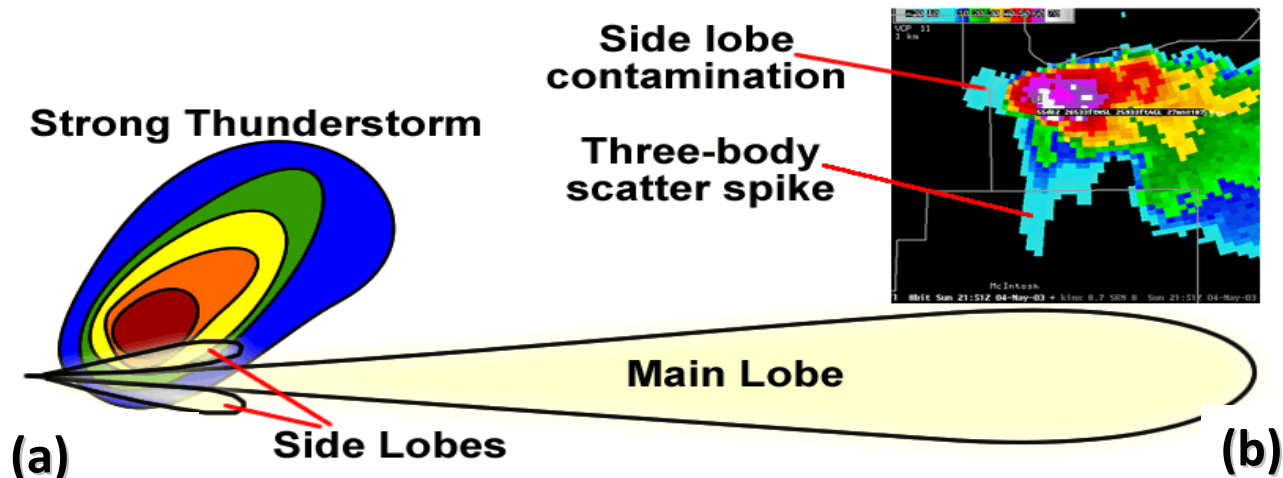


**Figure 2. (a) Conceptual example of conditions leading to sidelobe contamination. (b) Actual example from 4 May 2003 showing sidelobe spike as well as TBSS [Radar located NNE of storm]. (WDTB 2010)**

The TBSS, on the other hand is an elongation of reflectivity down radial (away from the radar) from a strong core and usually has stronger returns than the sidelobe spike. The TBSS forms due to radar radiation reflecting off a strong precipitation core toward the ground, from the ground back to the precipitation core and back to the radar (Wilson and Reum 1988; Doviak and Zrníc 1993). Though both are sometimes seen together, the TBSS is more commonly observed.

It should be noted that while the current discussion focuses on sidelobe contamination as it pertains to radar reflectivity, the other base moments (radial velocity and spectrum width) also suffer from sidelobes. Piltz and Burgess (2009) provide a good example of sidelobe contamination in radial velocity. Furthermore, their source of sidelobe contamination results from strong reflectivity gradients in the vertical, and is a good reminder of the three-dimensionality of this problem. The goal of this paper is to explore the possible application of reflectivity sidelobe contamination in the presence of a strong horizontal reflectivity gradient to the detection of severe hail. The

desire is to provide the forecaster with an additional qualitative tool that may add confidence that severe hail is present.

### 3. Data and Methodology

For this study a simple methodology was used: identify cases where sidelobe spikes were observed and match whether or not severe hail was observed before, during, or after the sidelobe spike occurred. Ground truth hail reports were obtained from both the national Climactic Data Center's *Storm Data* and the Severe Hazards Analysis and Verification Experiment (Ortega, et al. 2009). This study contains only a small number of observed sidelobe events, which were primarily observed by the authors. The data set contains 10 observed sidelobe spikes from nine different radars and over six different days (Table 1). The hail reports were examined to see if hail sizes exceeded severe thresholds, and the times of occurrence of severe hail if it occurred. Radar data was examined to record the time the first sidelobe spike appears and the first elevation in which it was observed, (Figures 3 and 4) and then the last time/elevation that the sidelobe spike was seen. A simple tally was performed of whether severe hail occurred prior to the

first sidelobe spike, between the first and last occurrence of any sidelobe spikes, or after the last occurrence of the sidelobe spike. Finally, the existence or non-existence of a TBSS was also recorded.

Date	Radar	VCP
20080728	KICT	212
20080728	KVNX	11
20090709	KFSD	212
20090718	KFDX	12
20090722	KUEX	12
20090722	KDMX	12
20090722	KDMX	212
20090723	KPUX	12
20090724	KDVN	12/212
20090724	KARX	212

**Table 1. List of events where sidelobe spikes were observed, including date, radar site, and VCP(s) used during the time that the sidelobe spike was present.**

#### 4. Results

From the 10 cases observed, every case but one had severe hail associated with a sidelobe spike. The signatures were observed between 46 km and 166 km in range from the radar, with a mean range of 97.1 km. The longest observed sidelobe spike lasted over 86 minutes and the shortest lasted less than two minutes. The mean observed time for sidelobe spikes for the data set was just under 35 minutes. Half of the radars were in VCP 212, four were in VCP 12 and one was in VCP 11. While the majority of the radars were scanning with a “Super-Res” VCP, half of the observed sidelobe spikes were seen in batch tilts, meaning that they were observed in legacy (1 deg azimuth x 1 km range) resolution (Figures 3 and 4). Only one case out of the 10 failed to exhibit a definitive TBSS (Table 2).

#### 5. Discussion

The TBSS has long been associated with the presence of severe hail within a thunderstorm and has been encouraged to be used as a “sufficient but not necessary condition for large hail identification” (Lemon 1998b). Though the TBSS likely indicates hail within the storm, Ortega, et al. (2010) shows only moderate skill for the TBSS (for all lead times) associated with severe hail found at the surface. Initial results from this sidelobe spike study, however, suggest that the presence of a sidelobe spike may be a strong indicator that severe hail is reaching the surface, though the authors urge caution in relying too heavily on these initial results. Though an intriguing start, much more research needs to be conducted before considering sidelobe spike identification a definitive hail detection technique.

There are a number of factors that may limit the effectiveness of utilizing the sidelobe spike in operational use, and the forecaster must consider these. When multiple storms are in the same area, sidelobe spikes may not be seen since radar echo from neighboring storms may decrease the reflectivity gradient needed to produce sidelobe contamination. The current sample of observations is too limited to give any sort of confidence on range dependency.

More study is needed to determine what effects various clutter suppression techniques employed by the WSR-88D have on side-lobe spike detection. It was surprising to find that half of the cases where side-lobe spikes were observed were with legacy resolution data. It is encouraging that forecasters can still see these signatures in the upper tilts of the radar, or at sites (such as DOD operated NEXRAD locations) that may still be limited to legacy resolution data at all tilts.

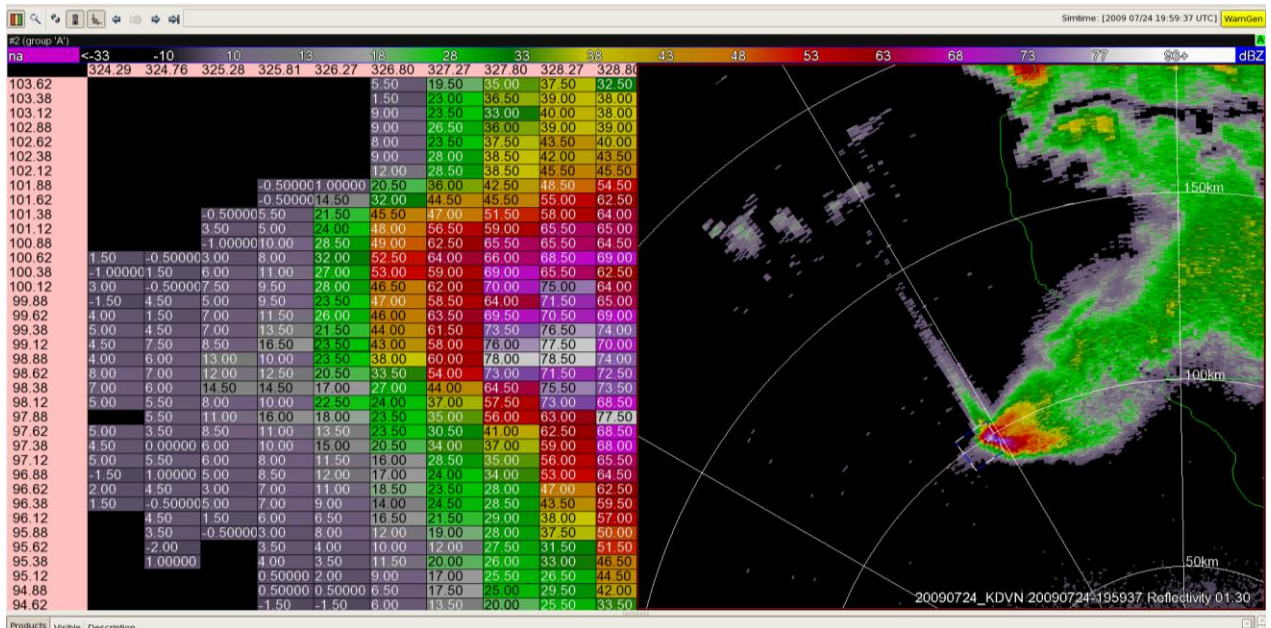


Figure 3. Radar reflectivity from KDVN on 24 July 2009 at 1.3 degrees elevation displaying both a TBSS and a sidelobe spike (right), and associated azimuth (X-axis top) vs range (Y-axis) table of gate values (historically known as a “B-scan”) (left) to better illustrate the reflectivity gradient. Note that since this is at 1.3 degrees elevation, the resolution of the radar data is 0.5 degrees in azimuth

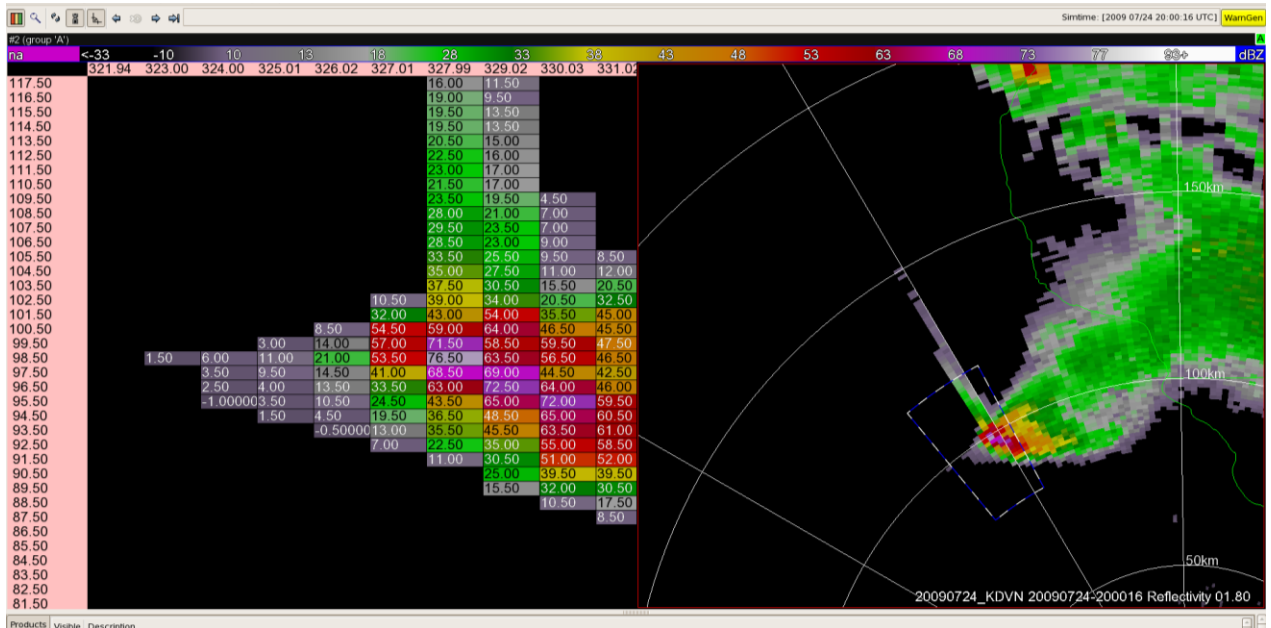


Figure 4. Same as in Figure 3 except at the next higher elevation scan. This illustrates how the sidelobe spike might appear in legacy resolution

Date	Radar	Resolution	SVR Hail Any Time?	Time of first side lobe (UTC)	Distance to radar (km)	TBSS	Time of last sidelobe (UTC)	Distance to radar (km)
20080728	KICT	legacy	D	22:35:41	65	Yes	23:35:00	64
20080728	KVNX	legacy	D	22:41:06	63	Yes	23:19:28	63
20090709	KFSD	legacy	P	19:21:32	62	No	19:31:36	65
20090718	KFDX	legacy	P	0:14:57	99	Yes	1:41:20	46
20090722	KUEX	super	P	19:39:04	75	Yes	20:18:31	52
20090722	KDMX	super	D	22:47:44	152	Yes	23:01:40	145
20090722	KDMX	super	P	23:33:35	122	Yes	23:34:54	120
20090723	KPUX	legacy	U	19:40:49	114	Yes	19:49:18	112
20090724	KDVN	super	P	19:20:49	131	Yes	20:13:24	86
20090724	KARX	super	P	19:29:19	140	Yes	20:07:14	166

**Table 2. Results from the 10 observed cases. Sidelobe detection was tracked from the first appearance at any elevation scan to the last appearance at any elevation scan. Though most of the radars were operating in a super-resolution capable volume coverage pattern, about half of the sidelobe spikes were mainly observed in the batch-cut tilts where the elevation scans revert to legacy resolution. P- severe hail prior to visible sidelobe spike; D – during visible sidelobe spike; U – unknown severe hail fell**

## 6. Conclusion

Forecasters use a mix of quantitative algorithms and qualitative feature identification techniques to aid in diagnosing severe weather potential from thunderstorms. Each of these tools have strengths and weaknesses, but are often used in conjunction with each other to increase the forecaster’s confidence in whether a particular storm is likely to produce heavy rain, hail and tornadoes. Sidelobe contamination in radar data occurs when there are strong horizontal (or vertical) gradients of reflectivity, on the order of 40 dB deg<sup>-1</sup>. This type of gradient is usually only seen in strong thunderstorms capable of producing hail. This study, though very limited in the number of observed cases, appears to show a strong relationship between the presence of a sidelobe spike and the occurrence of severe hail at the ground. The TBSS, also a good indicator of the presence of large hail, has a false alarm ratio of generally greater than 0.4. Identifying sidelobe spikes may aid in reducing false alarm rate and increase probability of detection when used as an additional interrogation tool. The gross

results shown are encouraging enough to continue to pursue studying this feature further.

It is unclear, as of the time of this study, what effect the sensitivity loss resulting from the dual-pol upgrade to the NEXRAD network will have on the ability to observe sidelobe spikes. This will be simulated soon and updated in supplementary material. It should be noted, however, that even if the ability to detect sidelobe spikes is no longer possible after the dual-pol upgrade, the additional dual-pol variables have proven to be able to lead a forecaster to confidently detect the presence of hail, and hopefully will show promise in distinguishing severe hail with additional research.

## 7. Acknowledgements

Much appreciation goes to the reviewers of this paper, in particular Dr. Rodger Brown.

This conference paper was prepared with funding provided by NOAA/Office of Oceanic and Atmospheric Research under NOAA-University of Oklahoma Cooperative

Agreement #NA17RJ1227, U.S. Department of Commerce. The statements, findings, conclusions, and recommendations are those of the author(s) and do not necessarily reflect the views of NOAA or the U.S. Department of Commerce.

## 8. References

- Bringi, V. N. and V. Chandrasekar, 2001: *Polarimetric Doppler Weather Radar: Principles and Applications*. Cambridge University Press, 636 pp.
- Brown, Rodger A., B. A. Flickinger, E. Forren, D. M. Schultz, D. Sirmans, P. L. Spencer, V. T. Wood, C. L. Ziegler, 2005: Improved Detection of Severe Storms Using Experimental Fine-Resolution WSR-88D Measurements. *Wea. Forecasting*, **20**, 3–14.
- Burgess, D. W., 1976: Single-Doppler radar vortex recognition. Part I: Mesoscale signatures. Preprints, *17th Conf. on Radar Meteorology*, Seattle, WA, Amer. Meteor. Soc., 97–103.
- Crum, T. D., and R. L. Alberty, 1993: The WSR-88D and the WSR-88D Operational Support Facility. *Bull. Amer. Meteor. Soc.*, **74**, 1669–1687.
- Donaldson, R. J., 1970: Vortex signature recognition by a Doppler radar. *J. Appl. Meteor.*, **9**, 661–670.
- Doviak, R. J. and D. S. Zrnić, 1993: *Doppler Radar and Weather Observations*. 2d ed. Academic Press, 562 pp.
- Federal Handbook, 2005: Federal Meteorological Handbook No. 11, Doppler Radar Meteorological Observations, Part B, 219 pp. [Available online at <http://www.ofcm.gov/fmh11/fmh11B.htm>.]
- Lemon, L. R., 1998a: Updraft identification with radar. Preprints, *19th Conf. Severe Local Storms*, Minneapolis, MN, Amer. Meteor. Soc., 709-712.
- Lemon, L. R., 1998b: The radar “three-body scatter spike”: An operational large-hail signature. *Wea. Forecasting*, **13**:327–340. doi: 10.1175/1520-0434(1998)013<0327:TRTBSS>2.0.CO;2
- Ortega, Kiel L., T. M. Smith, K. L. Manross, A. G. Kolodziej, K. A. Scharfenberg, A. Witt, J. J. Gourley, 2009: The Severe Hazards Analysis and Verification Experiment. *Bull. Amer. Meteor. Soc.*, **90**, 1519–1530. doi: 10.1175/2009BAMS2815.1
- Ortega, K. L., T. Meyer, J. Erlingis, and T. Smith, 2010: Evaluating Hail Detection Techniques with High-Resolution Hail Reports . 35<sup>th</sup> *National Weather Association Annual Meeting*, Tucson, AZ, USA, National Weather Association, xx-xx.
- Piltz, S. F. and D. W. Burgess, , 2009: The impacts of thunderstorm geometry and WSR-88D beam characteristics on diagnosing supercell tornadoes. *Extended Abstracts, 34th Conference on Radar Meteorology*, Williamsburg, VA, USA, AMS, P6.18. [<http://ams.confex.com/ams/pdfpapers/155944.pdf>]
- Stumpf, Gregory J., A. Witt, E. D. Mitchell, P. L. Spencer, J. T. Johnson, M. D. Eilts, K. W. Thomas, D. W. Burgess, 1998: The National Severe Storms Laboratory Mesocyclone Detection Algorithm for the WSR-88D\*. *Wea. Forecasting*, **13**, 304–326. doi: 10.1175/1520-0434(1998)013<0304:TNSSLM>2.0.CO;2

- Wilson, James W., D. Reum, 1988: The Flare Echo: Reflectivity and Velocity Signature. *J. Atmos. Oceanic Technol.*, **5**, 197–205. doi: 10.1175/1520-0426(1988)005<0197:TFERAV>2.0.CO;2
- Warning Decision Training Branch (WDTB), 2010. Distance Learning Operations Course (DLOC): Topic 3 Lesson 1 Section 5-2 Sidelobe Contamination. [<http://wdtb.noaa.gov/courses/dloc/topic3/lesson1/Section5/Section5-2.html>]
- Witt, Arthur, M. D. Eilts, G. J. Stumpf, J. T. Johnson, E. D. Mitchell, K. W. Thomas, 1998: An Enhanced Hail Detection Algorithm for the WSR-88D. *Wea. Forecasting*, **13**, 286–303. doi: 10.1175/1520-0434(1998)013<0286:AEHDAF>2.0.CO;2